RC23625 (W0506-042) June 6, 2005
Electrical Engineering

IBM Research Report

Losses Caused by Roughness of Metallization in Printed-Circuit Boards

A. Deutsch, C. Surovic, R. Krabbenhoft[1], G. V. Kopcsay, B. Chamberlin[2]
IBM Research Division
Thomas J. Watson Research Center
P.O. Box 218
Yorktown Heights, NY 10598

[1]IBM Server Group
Rochester, MN 55901

[2]IBM Microelectronics Division
Endicott, NY 13760

Losses Caused by Roughness of Metallization in Printed-Circuit Boards

A. Deutsch, C. Surovic, R. Krabbenhoft, G. V. Kopcsay, B. Chamberlin
IBM T. J. Watson Research Center, 1101 Kitchawan Road, Yorktown heights, NY 10598
Phone: (914) 945-2858, Fax: (914) 945-2141, email: deutsch@us.ibm.com
IBM Server Group, Rochester, MN 55901
IBM Microelectronics Division, Endicott, NY 13760

Abstract – In this paper the effect of metal roughness on the total loss, the extracted tanδ, and signal integrity of typical interconnections found in printed-circuit boards is extracted from measurements on three different materials. The differing characteristics of the roughened metal cross sections is highlighted, and a simplified, practical, two-dimensional, causal, broadband modeling methodology is shown.

Introduction

It has been shown by many researchers that the increase in the data-rates propagated on interconnections used on printed-circuit boards requires more accurate and causal transmission-line models for predicting system performance. The random data-patterns encountered on long signal paths have very fast risetimes commensurate with data-rates of 2-10 Gbps, in the order of 30-200 ps. At the same time, the long spans of steady-state levels caused by adjacent 0's or 1's require broadband causal models over the range DC to about 50 GHz. Such models need to accurately account for resistive and dielectric losses. Non-causal models can cause inaccurate signal integrity and timing prediction and circuit simulator convergence problems. Printed-circuit board fabricators are hard at work developing lower loss insulator materials to make the high data-rates possible. It is important to accurately separate the resistive and dielectric losses for these new materials and to extract the material characteristics over the entire frequency range of interest. Single value dielectric constant $\varepsilon_r^{'}$ and dielectric loss $\tan\delta$ supplied by vendors today cannot be used to generate broadband causal models. In addition, when used in system performance evaluations, erroneous predictions would occur as shown in Figs. 1 and 2. Three cases are compared, namely, with the use of broadband complex permittivity ε(ω), with constant $\varepsilon_r^{'}$ and no dielectric loss, and with constant $\varepsilon_r^{'}$ and constant tanδ. Even though the total attenuation in Fig. 1 with single value $\varepsilon_r^{'}$ and tanδ agrees fairly well at a target 3 GHz frequency with the broadband model, when used in actual simulations in Fig. 2, for a 3 Gbps signal and 76 cm long line, it is found that the actual propagated signals are quite different.

In this study, three different insulator materials were used to build the same card design. In each case, two cards were fabricated, with and without roughened metallization, and the total loss was extracted over the range 10 KHz to 50 GHz. This paper will show how significant the loss due to roughness is, how it affects the accuracy of the model generation, the signal integrity, the board fabrication development, and the difficulty in modeling this effect.

Test Vehicle Configurations

The same design was used for all the three different printed-circuit board materials used, namely A, B, and C. A single stripline with additional top and bottom pad layers form a total thickness of under 635 μm (25 mil). 100-μm (4.0 mil) wide, 32-μm (1.26 mil) thick single lines are attached to very small surface pads through 203-μm (8-mil) diameter vias. The design is optimized to reduce the discontinuities introduced by pads, vias, and probes at the ends of the signal lines as explained in [1]. The build for the card materials C and B were duplicated with and without roughened copper metallization. Card A was built with the standard process and with a very low profile roughening. Some typical profiles are shown in Fig. 3 for signal and ground plane layers for materials B, C, and A. The important part to notice is the difference in rough ridge profile between signal layer and ground layer, and between cards. Each card was made by a different manufacturer. Material A profile is shown in the bottom. Notice the ridges on the side of the signal lines in addition to the top and the very high irregularity on the ground plane in this case. Fig. 4 shows a very close view of the ridge tips. It can be seen that micro-nodules are electroplated that could be in size from 0.1 to 1 μm to promote adhesion. This increases surface area without adding to the overall topography. In addition, the side of the ridges and the conductor outline could have a thin layer of an organo-metallic compound. This will differ depending on whether the manufacturer used standard, reverse, or dual treatment. It is explained in [2-3] that standard treatment would be applied to the toothed, or non-drum side of the copper foil and was generally used on the three cards shown here. Fig. 4 also shows a typical view of this alloy layer. The metals that are used can have resistivity that is more than an order of magnitude higher than copper.

Eight cross sections were taken at various positions along the lines and one parallel to the length of the lines. It was found that for the card A, the low profile, LP, case, had the ridge height in the range of 2.5-5 μm, and for the rough case, 7.5-10 μm. For card B, the rough signal layer had ridges that were on the average 7.5 μm tall and 8 μm wide. The ground layer had 5.5 μm heights and 7.4 μm widths. For card C, the signal layer had heights of 5.3 μm and widths of 10.3 μm and for the ground layer, heights of 7.5 μm and widths of 8.6 μm. For typical copper resitivity of 2 μΩcm, skin-depth is in the range of 1.03 to 0.36 μm for 5 GHz to 40 GHz. This means, that the dimension of the ridges are larger than the skin-depth and the current will follow the contour of the ridges and increase the effective resistance and inductance and slow-down the wave propagation.

The higher resistivity coating on the surface of the ridges will exacerbate this effect. Moreover, the irregularity of the random ridges could generate some non-TEM components of the field longitudinally and further affect the wave propagation.

DC Analysis

The resistance, capacitance, and cross sectional dimensions were analyzed for all six cards in order to ensure that similar conditions were used for comparison and the data is shown in the Table. Given the fact that these parts came from three different manufacturers, it is believed that the results were quite close. Resistivity was obtained from cross sectional dimensions and four-point resistance measurements. Line capacitance and dielectric constants ε_r' were obtained at 1 MHz. ε_r' was obtained from measuring the capacitance of a 12.7-mm (500-mil) diameter circular plate placed on the signal layer. It is observed that the effective DC resistivity increased only in the range of 0.05 – 0.6%. The effective dielectric constant increased by 2.4-4.3% at 1 MHz. Card B had the largest area difference between smooth and rough cards, namely 8.6%. The other two had very similar dimensions with ΔArea = 1.9-4.8%. The resultant line capacitance changed by only 1.2-3.1% due to roughness. If the cross section is slightly smaller and the dielectric constant is slightly higher, the resultant capacitance will not change too much unless the effect of roughness is significant. This did not seem to be the case. In all cases, an average line cross section was assumed through the middle of the rough ridges. In summary, the Table shows that the effect of roughness on effective DC resistivity and low-frequency effective dielectric constant are very small. This was also confirmed by measuring the characteristic impedance, Z_o, in TDR,. The impedance values for rough and smooth cards were within 1%.

Extraction of Total Loss

It was shown in [1] that a short-pulse propagation time-domain technique combined with signal processing and iterative fitting and modeling can successfully extract the total loss for representative stripline interconnects over the range 10 KHz to 50 GHz. It relies on a carefully built representative test vehicle that minimizes the interface discontinuities but retains all the key processing steps of an actual multi-layer card. High-bandwidth time-domain instrumentation and accessories are used such as the Agilent 86100B sampling oscilloscope with an 86118A, 70 GHz, detector unit connected through 65 GHz cables and coaxial probes (such as 67A from GGB Industries). In addition, the Picoseconds Pulse Labs 4022 TDT Source Pulse Enhancer and 5206 Differentiator allow the generation of 11 ps risetime step and 20 ps wide pulse excitations. The 20-ps wide short pulse is launched on two identical lines of different lengths. Signal processing combined with iterative fitting and modeling based on a Debye model for the complex permittivity, $\varepsilon(f)$, allow the extraction of attenuation $\alpha(f)$ and phase constant $\beta(f)$ and the broadband $\varepsilon(f)$. Fig. 5 shows a typical comparison of measured and calculated attenuation for the smooth card C. In this case the measurement bandwidth was 2.2 GHz to 38 GHz and the Debye-model extrapolated the data over the 10 KHz to 50 GHz range.

Effect of Surface Roughness

In order to eliminate the effect of slight differences in cross section, resistivity, and dielectric constants, a common cross section with a trapezoidal shape of width 91.9 / 109 μm (3.62 / 4.29 mil) or effective 100.5 μm (3.955 mil) and thickness of 32.0 μm (1.26 mil) was used for all three materials. The dielectric heights were $h_1 = h_2 = 114.0$ μm (4.49 mil). In all three cases, the conditions for $R(f)$, $L(f)$, $C(f)$, and $G(f)$ calculations were such that the fit was either made to the total loss for the smooth cards or the total loss for the roughened cards, but the cross section was the same. The $\varepsilon_{r\ 1MHz}'$ and ρ_{DC} that were used were extracted from measurements of the six actual cards of this study. Fig. 6 then shows the resultant six attenuations. The solid traces correspond to the smooth cards. The low-loss materials A and B have a substantial increase in total loss due to roughness. At 5 GHz, A and B cards have an increase in attenuation of 49.8% and 20.3%, respectively. At 10 GHz, the increase is 53.4% and 23.6%. Material A with roughened metallization produces a total interconnect loss that is very close to the loss of card C which is a standard material in use today. All the advantages of lower tanδ are overwhelmed by the losses due to roughness. Material C, in fact, has the least increase due to the ridges, namely at 5 GHz, only 5.5% increase, and at 10 GHz, 10.6%. It is possible that the newer materials require a more aggressive roughening process.

The values shown in Fig. 6 for the roughened cards were calculated by assuming an average cross section through the rough ridges. What this implies is that when extracting the effective $\varepsilon_r'(f)$ and $\tan\delta(f)$, the effect of roughness which is an additional resistive loss, gets attributed to dielectric loss. This is because the actual topography of the ridges is not accounted for. As a result, the error in the extracted tanδ is quite large as shown in Fig. 7. This issue has also been highlighted in [4] and attempts have been made to find analytical techniques fitted to measurements to alleviate this error.

Modeling the Effect of Roughness

Including the actual profile of the ridges shown in Fig. 4 in any full-wave electromagnetic field solver can be extremely costly in the number of unknowns and run time. Attempts have been made to use stochastic techniques for the calculation of capacitance [5] and effective conductivity [6] but complete broadband causal model generation has not been attained. In this study, an attempt was made to continue using the two-dimensional field solver that was used for the smooth card analyses, such as CZ2D [7]. An equivalent cross section is shown in Fig. 8 for card B. 7.5 µm tall rectangles with 8 µm and 5 µm widths and 3 µm separations represented the ridges. Each rectangle had a 1 µm shell of material with resistivity of ρ = 15 µΩcm. The ridges on the ground layer were represented by a thin, 5.5 µm, layer with ρ = 15 µΩcm. The extraction was then performed for *C(f)* and *G(f)* by using the tanδ values obtained for the smooth card. For the case of card C, the equivalent cross section had uniform ridges with widths of 10 µm, heights of 5.5 µm, and resistivity of 2.086 µΩcm. The ground ridges were represented by a 7.5 µm thick layer with resistivity of ρ = 50 µΩcm. This type of a simplification can only be achieved if both the smooth and roughened versions of the same build are available. This can, however, alleviate very costly computations and provide fairly accurate, causal, predictive broadband models for system performance assessment.

Simulations were also performed for two representative data-rates, namely 3 Gbps and 6 Gbps, with and without roughness-induced loss. 333 ps and 166 ps wide pulses were transmitted on 76.2 cm and 38 cm long lines, respectively, with the card B wiring and the common cross section described earlier for Fig. 9. For the 3 Gbps case, the loss in useable length was 2.12 cm (2.8%), the loss in amplitude was 1.8%, and the delay increase was 95.6 ps or 1.9%. In the case of 6 Gbps, as shown in Fig. 9, the loss in useable length was 4 cm or 10.5%, the increase in delay was 44 ps or 1.8%, and the decrease in signal amplitude was 17.5%.

Conclusions

It has been shown that resistive losses caused by the roughening of metallization in printed-circuit board wiring can be quite significant. The increase of total loss ranged from 5.5% to 49.5%, even at 5 GHz. The use of roughness to promote adhesion can cancel the beneficial low dielectric loss characteristics of newly developed card insulators and manufacturers need to thrive to eliminate the rough ridges. The effect on signal integrity was shown to increase with frequency and could curtail the delivery of high-performance systems or increase system complexity and cost.

The most significant finding of the study was that this effect will be quite different in characteristic depending on material used by card manufacturer and treatment employed by supplier of metal foil. The rough ridge profile could even differ on the ground plane layer from the signal line layer within the same card cross section. The coating of the lines and the composition of the micro-nodules is not generally released or known by vendors and the effective resistivity can be significantly higher than for copper metallization. The resultant composite cross section cannot be predicted. Accurate three-dimensional modeling is prohibitive in computation cost. Even faster stochastic modeling approaches require cross sectional information which is hard to obtain. A practical approach that circumvents costly analyses was outlined in this paper. It relies on the availability of a smooth version of the card build for each material considered. This allows the use of fast, two-dimensional modeling techniques for generating causal, broadband, predictive models for simulation. The implicit assumption is that the two card constructions maintain the same insulator properties.

References

[1] A. Deutsch, T-M. Winkel, G. V. Kopcsay, C. W. Surovic, B. J. Rubin, G. A. Katopis, B. J. Chamberlin, R. S. Krabbenhoft, "Extraction of *ε(f)* and tanδ*(f)* for Printed-Circuit Board Insulators up to 30 GHz Using the Short-Pulse Propagation Technique", IEEE Trans. On Adv. Packg., vol. 28, no. 1, pp.4-9, Feb. 2005.

[2] http://www.gould.com/cf_jtc.htm

[3] B. L. Adams-Melvin, D. R. McGregor, K. H. Dietz, "Effects of Copper Foil Type and Surface Preparation on Fine Line Image Transfer in Primary Imaging of Printed Wiring Boards", digest PC World Convention VII, pp. 1-20, Basel, Switzerland, May 21-24, 1996.

[4] G. Brist, S. Hall, S. Clouser, T. Liang, "Non-Classical Conductor Losses Due to Copper Foil Roughness and Treatment", digest ECWC10 Conference at APEX IPC Printed Circuits Expo and Designers Summit 2005, pp. 1-11, Feb. 22-24, 2005, Anaheim, CA.

[5] Z. Zhu and J. White, "FastSies: a fast stochastic integral equation solver for modeling the rough surface effect" submitted to , ICCAD 2005.

[6] L. Proekt and A. C. Cangellaris, "Investigation of the Impact of Conductor Surface Roughness on Interconnect Frequency-Dependent Ohmic Loss", 2003 ECTC Conference, pp.1004-1010, June 2003, New Orleans, LA.

[7] W. T. Weeks, L. L. Wu, M. F. McAllister, and A. Singh, "Resistive and inductive skin effect in rectangular conductors", IBM. J. Res. And Dev., vol. 23, pp.652-660, 1979.

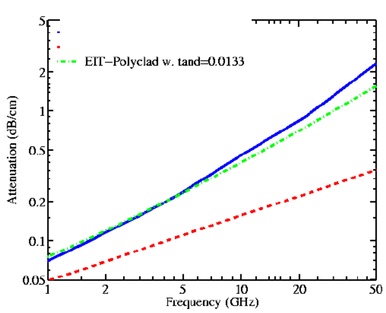

Fig. 1 Calculated attenuations for complex permittivity *ε(f)* (solid), constant ε_r and tanδ=0 (dashed), and constant ε_r and tanδ = 0.0133 (dot-dashed) for card B.

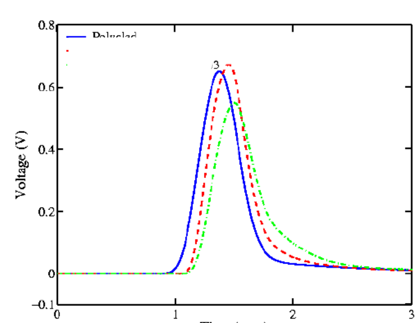

Fig. 2 Simulated 333-ps wide pulses (3 Gbps) propagated on 4x1.26 mil cross section lines for the three cases of Fig. 1.

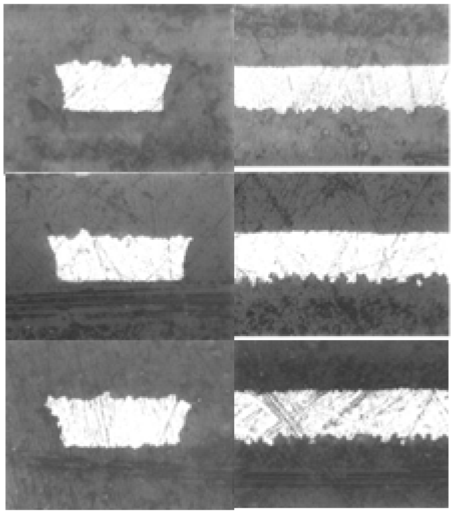

Fig. 3 Typical signal (left side) and ground-plane cross sections (right side) for cards B, C, and A.

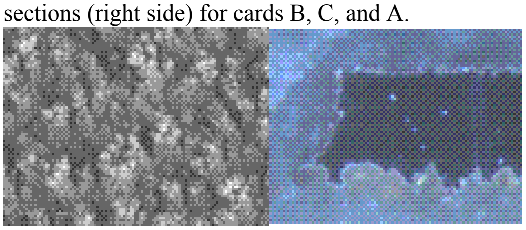

Fig. 4 Top view (left side) and coating of ridges (right side).

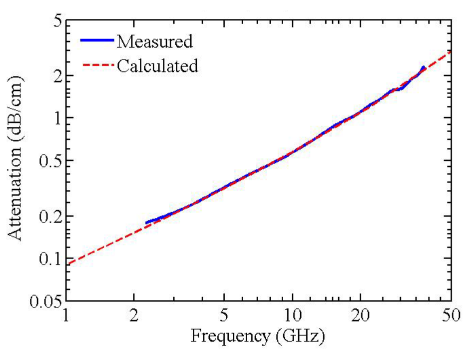

Fig. 5 Measured and calculated *α(f)* for smooth card C.

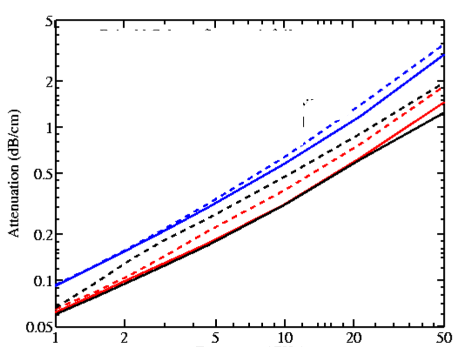

Fig. 6 Calculated attenuations for the three smooth (solid) and three roughened cards (dashed).

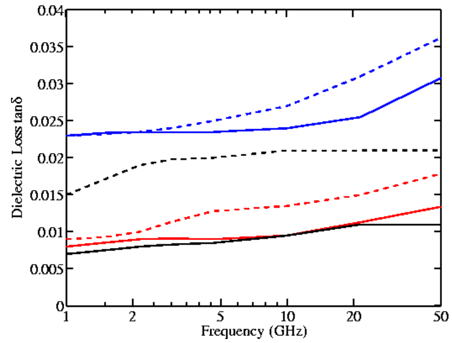

Fig. 7 Extracted dielectric loss for the six cases in Fig. 6.

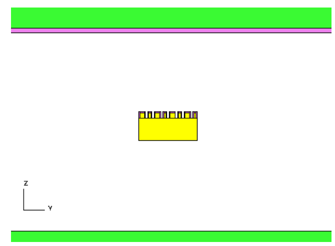

Fig. 8 Two-dimensional model used for roughened card B.

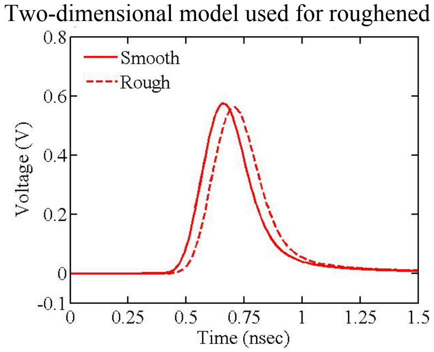

Fig. 9 Simulated 6 Gbps response for 38-cm long trace on card B with smooth (solid) and roughened (dashed) metallization.

TABLE

	Smooth	Rough	
Card A	**ρ = 2.096 μΩcm,**	**ρ = 2.097 μΩcm**	**Δ = 0.05%**
Card B	**ρ = 2.070 μΩcm,**	**ρ = 2.080 μΩcm**	**Δ = 0.50%**
Card C	**ρ = 2.073 μΩcm,**	**ρ = 2.086 μΩcm**	**Δ = 0.60%**
Card A	**ε_r = 3.45**	**ε_r = 3.60**	**Δ = 4.3%**
Card B	**ε_r = 3.55**	**ε_r = 3.70**	**Δ = 4.2%**
Card C	**ε_r = 4.10**	**ε_r = 4.20**	**Δ = 2.4%**
Card A	**R = 0.069 Ω/cm**	**R = 0.0725 Ω/cm**	**Δ = 5.07%**
Card B	**R = 0.080 Ω/cm**	**R = 0.0880 Ω/cm**	**Δ = 10.0%**
Card C	**R = 0.065 Ω/cm**	**R = 0.0670 Ω/cm**	**Δ = 3.00%**
Card A	**Area = 3038mm^2**	**Area = 2893mm^2**	**Δ = -4.8%**
Card B	**Area = 2592mm^2**	**Area = 2368mm^2**	**Δ = -8.6%**
Card C	**Area = 3184mm^2**	**Area = 3123mm^2**	**Δ = -1.9%**
Card A	**C_{mes} = 1.366 pF/cm**	**C_{mes} = 1.408 pF/cm**	**Δ = 3.1%**
Card B	**C_{mes} = 1.200 pF/cm**	**C_{mes} = 1.215 pF/cm**	**Δ = 1.3%**
Card C	**C_{mes} = 1.440 pF/cm**	**C_{mes} = 1.473 pF/cm**	**Δ = 2.3%**
Card A	**h = 106/95 μm**	**h = 103/97 μm**	
Card B	**h = 103/115 μm**	**h = 103/114 μm**	
Card C	**h = 103/137 μm**	**h = 111/133 μm**	